Posttranslational Modification of Pili upon Cell Contact Triggers *N. meningitidis* Dissemination

Julia Chamot-Rooke, *et al.*

Science **331**, 778 (2011);
DOI: 10.1126/science.1200729

M5313-derived and h-MCL induced higher IFN-β secretion than *L.g.*M− parasites or h-CL parasites (Fig. 2C). Furthermore, this expression was TLR3-TRIF dependent, with the MyD88 signaling pathway augmenting secretion (Fig. 2C).

Endosomal TLRs recognize nucleic acid motifs, with TLR7 and TLR3 recognizing single-stranded RNA (ssRNA) and double-stranded RNA (dsRNA), respectively (*23*). Our experimental evidence suggested that nucleic acid–derived motifs were involved in the host macrophage response to infection with metastasizing *L.g.* parasites. We observed increased production of CCL5, TNF-α, and IL-6 in macrophages exposed to single-stranded ribonuclease (ssRNAse)– and deoxyribonuclease (DNAse)–treated nucleic acids derived from *L.g.*M+ parasites, compared with *L.g.*M− and *L.major* LV39 (fig. S2). Although not statistically significant, these results suggested that the nucleic acid motif is resistant to ssRNAse and DNAse treatments and is likely to be dsRNA.

L.Viannia parasites, including *L.g.*M5313(M+) and *L. guyanensis* and *L. braziliensis* MCL human isolates, harbor the dsRNA *Leishmania RNA virus 1* (LRV1) (*24*–*26*). These viruses have a capsid coat protecting a 5.3-kb dsRNA genome (*27*). Metastasizing promastigotes had greater levels of LRV1 (*L.g.*M+ or h-MCL-LRV^{high}) than nonmetastasizing promastigotes (*L.g.*M− or h-CL-LRV^{low}) as shown by the presence of a ~5.3-kb, DNAse-insensitive, RNAse III–sensitive band in agarose gels, and LRV1 quantification by quantitative reverse transcriptase–polymerase chain reaction (qRT-PCR) (Fig. 3, A to C, and fig. S3A). We thus verified that macrophages treated with purified LRV1 dsRNA (fig. S3) induced a phenotype similar to that of macrophage infected with metastasizing parasites, and as shown by an increased expression of CXCL10, CCL5, TNF-α, IL-6, and IFN-β transcripts, this increase was TLR3 dependent (Fig. 3D). Because the *L.g.*M5313 M+ and M− parasites were not isogenic, we performed new experiments with parasites derived from the WHO reference strain *L.g.*M4147 that metastatizes in the hamster (*28*) and carries the LRV1-4 virus (*29*). Macrophage infection with *L.g.*M4147-LRV^{high} parasites produced significantly greater amounts of cytokines and chemokines than infection with its respective isogenic virus-free derivative *L.g.*M4147LRV^{neg}, in a TLR3-dependent manner (Fig. 3E and fig. S4) (*30*, *31*). Similar parasite burdens were observed for all parasites infected into the wild-type and the TLR-, TRIF-, and MyD88-deficient macrophages (table S1).

A role for TLR3 and LRV1 in leishmaniasis development was analyzed in vivo, with TLR3$^{-/-}$, TLR7$^{-/-}$, and WT mice that were infected in the footpad. A significant decrease in footpad swelling, and diminished parasite burden, were observed in TLR3$^{-/-}$ mice infected with *L.g.*M+LRV^{high} (M5313) or *L.g.*M4147–LRV^{high} parasites compared with wild-type mice (Fig. 4 and fig. S5). No consistent, significant decrease in disease pathology was observed between TLR3$^{-/-}$ and wild-type mice infected with *L.g.*M−LRV^{low} (Lg17) or *L.g.*M4147–LRV^{neg} or between TLR7$^{-/-}$ and wild-type infected mice with the different parasite isolates (Fig. 4 and Fig. S5). Further experimentation is required to elucidate the role of TLR7-dependent immune responses with respect to infection with LRV1-containing *Leishmania* parasites.

Our work showed that recognition of LRV1 within metastasizing *L.g.* parasites by the host promoted inflammation and subverted the immune response to infection to promote parasite persistence (*2*, *3*, *32*). Because recognition of LRV1 within the metastasizing *L.g.* parasites arises early after infection, we hypothesize that LRV1 dsRNA is released from dead parasites, unable to survive within the host macrophage. These results could open the door to better diagnosis of risk for MCL disease and facilitate the development of new and more efficient treatment regimes.

References and Notes

1. K. Weigle, N. G. Saravia, *Clin. Dermatol.* **14**, 433 (1996).
2. C. Vergel *et al.*, *J. Infect. Dis.* **194**, 503 (2006).
3. J. E. Martinez, L. Alba, *Trans. R. Soc. Trop. Med. Hyg.* **86**, 392 (1992).
4. A. Barral *et al.*, *Am. J. Pathol.* **147**, 947 (1995).
5. V. S. Amato, F. F. Tuon, H. A. Bacha, V. A. Neto, A. C. Nicodemo, *Acta Trop.* **105**, 1 (2008).
6. J. Arevalo *et al.*, *J. Infect. Dis.* **195**, 1846 (2007).
7. D. R. Faria *et al.*, *Infect. Immun.* **73**, 7853 (2005).
8. S. T. Gaze *et al.*, *Scand. J. Immunol.* **63**, 70 (2006).
9. C. Pirmez *et al.*, *J. Clin. Invest.* **91**, 1390 (1993).
10. D. A. Vargas-Inchaustegui *et al.*, *Infect. Immun.* **78**, 301 (2010).
11. J. M. Blackwell, *Parasitol. Today* **15**, 73 (1999).
12. L. Castellucci *et al.*, *J. Infect. Dis.* **194**, 519 (2006).
13. B. Travi, J. Rey-Ladino, N. G. Saravia, *J. Parasitol.* **74**, 1059 (1988).
14. J. E. Martínez, L. Valderrama, V. Gama, D. A. Leiby, N. G. Saravia, *J. Parasitol.* **86**, 792 (2000).
15. N. Acestor *et al.*, *J. Infect. Dis.* **194**, 1160 (2006).
16. Materials and methods are available as supporting material on *Science* Online.
17. C. Bogdan, M. Röllinghoff, A. Diefenbach, *Immunol. Rev.* **173**, 17 (2000).
18. F. H. Abou Fakher, N. Rachinel, M. Klimczak, J. Louis, N. Doyen, *J. Immunol.* **182**, 1386 (2009).
19. R. Ben-Othman, L. Guizani-Tabbane, K. Dellagi, *Mol. Immunol.* **45**, 3222 (2008).
20. K. A. Cavassani *et al.*, *J. Exp. Med.* **205**, 2609 (2008).
21. R. Le Goffic *et al.*, *PLoS Pathog.* **2**, e53 (2006).
22. K. S. Lang *et al.*, *J. Clin. Invest.* **116**, 2456 (2006).
23. S. L. Doyle, L. A. O'Neill, *Biochem. Pharmacol.* **72**, 1102 (2006).
24. L. Guilbride, P. J. Myler, K. Stuart, *Mol. Biochem. Parasitol.* **54**, 101 (1992).
25. G. Salinas, M. Zamora, K. Stuart, N. Saravia, *Am. J. Trop. Med. Hyg.* **54**, 425 (1996).
26. M. M. Ogg *et al.*, *Am. J. Trop. Med. Hyg.* **69**, 309 (2003).
27. T. L. Cadd, M. C. Keenan, J. L. Patterson, *J. Virol.* **67**, 5647 (1993).
28. J. A. Rey, B. L. Travi, A. Z. Valencia, N. G. Saravia, *Am. J. Trop. Med. Hyg.* **43**, 623 (1990).
29. G. Widmer, A. M. Comeau, D. B. Furlong, D. F. Wirth, J. L. Patterson, *Proc. Natl. Acad. Sci. U.S.A.* **86**, 5979 (1989).
30. L. F. Lye *et al.*, *PLoS Pathog.* **6**, e1001161 (2010).
31. Y. T. Ro, S. M. Scheffter, J. L. Patterson, *J. Virol.* **71**, 8991 (1997).
32. A. Barral *et al.*, *Am. J. Trop. Med. Hyg.* **53**, 256 (1995).

33. We are grateful to N. Saravia (CIDEIM, Colombia) and Instituto Oswaldo Cruz, for *L. guyanensis* strains; S. Akira (Frontier Research center, Osaka University), P. Romero (LICR, Lausanne), and B. Ryffel (CNRS, Orléans) for knockout and mutant mice; M. Delorenzi (SIB, Lausanne) for bioinformatics expertise; F. Morgenthaler (Cellular Imaging Facility, Lausanne), S. Cawsey, and M.-A. Hartley for technical assistance; and J. Patterson and Y. T. Ro for the *L.g.*M4147 strains. This work was funded by FNRS grants 3100A0-116665/1 (N.F.) and 310030-120325 (P.L.), Foundation Pierre Mercier (S.M.), and NIH A129646 (S.M.B.). Microarray data are available within the Gene Expression Omnibus database (GSE21418) and at http://people.unil.ch/nicolasfasel/data-from-fasels-lab/.

Supporting Online Material

www.sciencemag.org/cgi/content/full/331/6018/775/DC1
Materials and Methods
Figs. S1 to S4
Table S1
References

20 October 2010; accepted 23 December 2010
10.1126/science.1199326

Posttranslational Modification of Pili upon Cell Contact Triggers *N. meningitidis* Dissemination

Julia Chamot-Rooke,[1,2] Guillain Mikaty,[3,4] Christian Malosse,[1,2] Magali Soyer,[4,5] Audrey Dumont,[4,5] Joseph Gault,[1,2] Anne-Flore Imhaus,[4,5] Patricia Martin,[3,4] Mikael Trellet,[6] Guilhem Clary,[4,7,8] Philippe Chafey,[4,7,8] Luc Camoin,[4,7,8] Michael Nilges,[6] Xavier Nassif,[3,4,9] Guillaume Duménil[4,5]*

The Gram-negative bacterium *Neisseria meningitidis* asymptomatically colonizes the throat of 10 to 30% of the human population, but throat colonization can also act as the port of entry to the blood (septicemia) and then the brain (meningitis). Colonization is mediated by filamentous organelles referred to as type IV pili, which allow the formation of bacterial aggregates associated with host cells. We found that proliferation of *N. meningitidis* in contact with host cells increased the transcription of a bacterial gene encoding a transferase that adds phosphoglycerol onto type IV pili. This unusual posttranslational modification specifically released type IV pili-dependent contacts between bacteria. In turn, this regulated detachment process allowed propagation of the bacterium to new colonization sites and also migration across the epithelium, a prerequisite for dissemination and invasive disease.

The Gram-negative bacterium *Neisseria meningitidis* is a leading cause of septicemia and meningitis in humans (*1*). Initially, individual bacteria adhere to the nasopharynx epithelium via their type IV pili, a filamentous organelle common to numerous pathogenic bac-

terial species (*2*). In the following hours, bacteria proliferate on the cellular surface in tight three-dimensional aggregates termed microcolonies. The formation of these aggregates results from homotypic, type IV pili–mediated contacts between the bacteria themselves and contacts between bacteria and the host cell plasma membrane. Contacts with host cells are enhanced by the formation of bacteria-induced plasma membrane protrusions (*3*). After this proliferation phase, individual bacteria are thought to detach from the microcolonies, leading to propagation to new hosts and dissemination throughout the body in case of invasive infection. Understanding the molecular mechanisms underlying the life cycle of *N. meningitidis* is a key step toward identification of prevention and treatment strategies of meningococcemia. The major component of *Neisseria* spp. type IV pili (PilE or pilin) is modified with phosphocholine (PC), phosphoethanolamine (PE), or phosphoglycerol (PG) (*4*–*6*). We wanted to determine the impact of these unusual posttranslational modifications (PTM) on the pathogenesis of *N. meningitidis*.

A whole-protein mass spectrometry approach was chosen to determine the phosphorylation state of type IV pili (*7*, *8*). Analysis of purified pili from the well-characterized 8013 strain (*9*) grown on solid medium (*10*) yielded a main peak with a mass of 17,491 daltons and a minor secondary peak with a mass of 17,645 daltons (Fig. 1A) corresponding to the addition of one PG (154 daltons, fig. S1A). Analysis of purified pili from strains carrying point mutations substituting conserved serine residues 69 and 93 of the PilE protein with alanines (Fig. 1, B and C) showed that all pilin subunits were modified with PG on Ser69 (17,491 daltons), whereas only about 15% of pilin subunits were also modified on Ser^{93} (17,645 dalton). The *NMV_0885* gene (ortholog of *NMA1705* and *NMB1508*) was a good candidate to carry out this activity because it is part of the cluster of orthologous group (COG) titled phosphoglycerol transferase and related proteins (COG1368, fig. S1C) (*11*). Analysis of type IV pili purified from a strain carrying a deletion in the *NMV_0885* gene revealed a single peak of 17,337 daltons that corresponds to pilin without any PG (Fig. 1D), demonstrating that this gene is responsible for the transfer of PG onto the pilin. We thus named the transferase PptB (pilin phosphotransferase B).

The *pptB* gene was previously described as a member of a group of 16 *N. meningitidis* genes containing a two-component system-regulated promoter referred to as CREN for contact regulatory element of *Neisseria* (*12*–*14*). Transcription of *pptB* increased two- to threefold over a period of 4 hours after adhesion to epithelial cells (*12*), suggesting that modification of type IV pili with PG could be triggered upon contact with host cells. To test this possibility, we expressed the *pptB* gene under the transcriptional control of the isopropyl-β-D-thiogalactopyranoside (IPTG)–inducible *lac* promoter to mimic the threefold induction found on host cells (Fig. 2A). In the presence of inducer, the peak corresponding to two PG modifications (17,645 daltons) became the most abundant form (Fig. 2, B and C, and fig. S2). Substitution of Ser^{93} into an alanine (S93A) (Fig. 2D) indicated that Ser^{93} is the main phosphorylation site upon induction of *pptB*, whereas Ser^{69} phosphorylation level remained constant. The expression level of the *pptB* gene thus determines the phosphorylation level of the pilin subunits on Ser^{93}.

We used two-dimensional gel electrophoresis followed by immunoblot to demonstrate increased modification of pilin with the negatively charged PG while bacteria were proliferating in contact with host cells. Analysis of PilE from bacteria growing in suspension displayed a major spot with an isoelectric point around 6 (fig. S3). Upon incubation with host cells, spots corresponding to acidic forms appeared after 2 and 4 hours. Pilin isoelectric point changes did not occur in the *pilES93A*-expressing strain. Thus, after *pptB* transcriptional increase upon contact with host cells, the isoelectric point of a significant proportion of the major pilin subunit became more acidic after modification of Ser^{93}.

To gain insight into the potential impact of this modification, we modeled the three-dimensional structure of the pilin from *N. meningitidis* with and without PG on Ser^{93} based on the known *N. gonorrhoeae* pilin structure and energy minimization in the context of the pilus fiber (Fig. 2E). Ser^{93} is surrounded by five lysine residues (Fig. 2F), a positively charged patch postulated to be important in type IV pili function (*15*). Modification of Ser^{93} with PG introduces a

[1]Ecole Polytechnique, Laboratoire des Mécanismes Réactionnels, Palaiseau F-91128, France. [2]CNRS, UMR7651, Palaiseau F-91128, France. [3]INSERM, U1002, Paris F-75015, France. [4]Université Paris Descartes, Faculté de Médecine Paris Descartes, Paris F-75006, France. [5]INSERM, U970, Paris Cardiovascular Research Center, Paris F-75015, France. [6]Unité de Bioinformatique Structurale, Unité de Recherche Associée CNRS 2185, Institut Pasteur, Paris F-75015, France. [7]Institut Cochin, CNRS (UMR 8104), Paris F-75014, France. [8]INSERM, U1016, Paris F-75014, France. [9]Assistance Publique–Hôpitaux de Paris, Hôpital Necker–Enfants Malades, Paris F-75015, France.

*To whom correspondance should be addressed. E-mail: guillaume.dumenil@inserm.fr

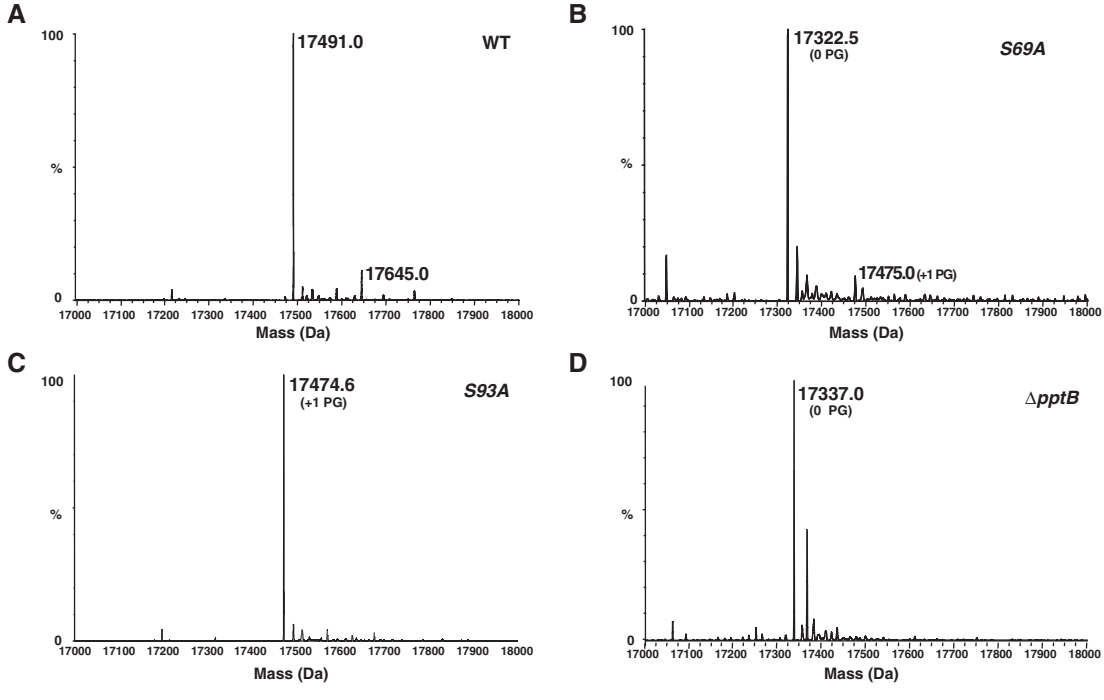

Fig. 1. Modification of the pilin subunit with PG by the PptB transferase. Whole-protein mass spectrometry analysis of type IV pili purified from the wild-type strain (WT) (**A**), from a strain harboring a S69A mutation in the *pilE* gene (**B**), from a strain harboring a S93A mutation in the *pilE* gene (**C**), and from a mutant in the *NMV_885* gene (Δ*pptB*) (**D**).

negative charge carried by the PG group protruding from the pilus structure (Fig. 2G and fig. S4). Modeling of bundles of four antiparallel pili fibers showed that the average interaction energy was largely favorable (60 kcal difference) for the pili with no modification on Ser[93] when compared with the same structure with a PG on Ser[93] (Fig. 3, A to C). Thus, modification of Ser[93] with PG would strongly destabilize fiber interaction, suggesting that this PTM could have important consequences for type IV pili function.

We addressed the functional role of this PTM in key steps of *N. meningitidis* pathogenesis. Pilin modification with PG did not have any effect on the amount of type IV pili present on the bacterial surface (fig. S5, A and B). In contrast, as predicted by molecular modeling, ultrastructural analysis by negative staining showed that increased pilin modification with PG blocked the formation of bundles of pili (Fig. 3D). In the wild-type strain, pili bundles were commonly about 30 nm wide, thus containing several 6- to 8-nm-wide individual fibers (Fig. 3D). Upon transcriptional induction of the *pptB* gene, only thin fibers having the expected size of individual pili could be found (Fig. 3D and fig. S5C). Increased modification of pilin with PG thus blocks bundle formation.

Type IV pili bundle formation and *N. meningitidis* aggregation are linked (*16*). *pptB* gene deletion or the S93A substitution led to increased aggregate formation in suspension (Fig. 3E) and consistently increased transcription of the *pptB* gene abrogated bacterial aggregation (Fig. 3F). The effect of increased *pptB* transcription on aggregation was rescued by the S93A point mutation (Fig. 3G). Increased modification of Ser[93] with PG thus strongly reduces type IV pili–dependent bacterial aggregation by introducing a negative charge at this site (fig. S6B). This anti-aggregative effect appeared to overcome the pro-aggregative activity of the minor pilin PilX (fig. S6, C and D).

The effect of pilin modification with PG on adhesion to epithelial cells was evaluated. The first step of adhesion, which is the contact of individual bacteria with the cell surface (Fig. 4A), occurred independently of the level of glycerophosphorylation (Fig. 4B). Bacterial microcolonies formed by the strains affected in pilin modification with PG did not appear morphologically different from the wild-type multilayered microcolonies (Fig. 4C). Furthermore, pilin glycerophosphorylation had little effect on the total number of cell-associated bacteria after 6 hours (Fig. 4D). To investigate the effect of

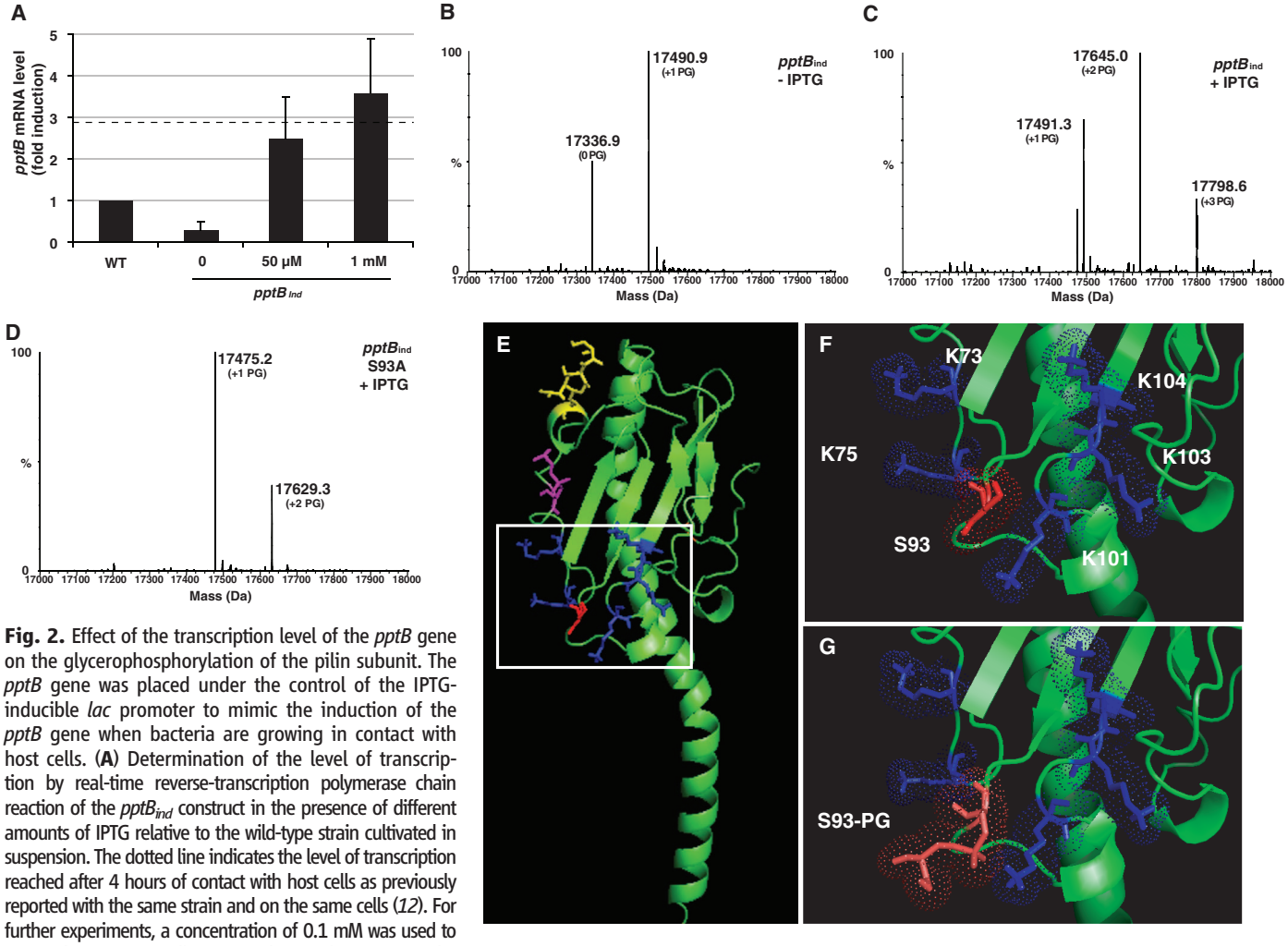

Fig. 2. Effect of the transcription level of the *pptB* gene on the glycerophosphorylation of the pilin subunit. The *pptB* gene was placed under the control of the IPTG-inducible *lac* promoter to mimic the induction of the *pptB* gene when bacteria are growing in contact with host cells. (**A**) Determination of the level of transcription by real-time reverse-transcription polymerase chain reaction of the $pptB_{ind}$ construct in the presence of different amounts of IPTG relative to the wild-type strain cultivated in suspension. The dotted line indicates the level of transcription reached after 4 hours of contact with host cells as previously reported with the same strain and on the same cells (*12*). For further experiments, a concentration of 0.1 mM was used to mimic the effect of cell contact. The graph represents the mean ± SEM of three independent experiments. (**B**) Whole-protein mass spectrometry analysis of the pilin subunit purified from the $pptB_{ind}$ strain in absence of IPTG and therefore with low amounts of PptB ($pptB_{ind}$ − IPTG). (**C**) Effect of increased *pptB* level after induction of the $pptB_{ind}$ construct with 0.1 mM IPTG on pilin mass ($pptB_{ind}$ + IPTG). (**D**) Analysis of the pilin subunit containing the S93A substitution in the $pptB_{ind}$ strain in presence of 0.1 mM IPTG ($pptB_{ind}$ S93A + IPTG). (**E**) Molecular modeling of the *N. meningitidis* pilin monomer with the PTMs found when bacteria are grown in suspension: GATDH (glyceramido tri-deoxy hexose) sugar modification on Ser[63] (yellow) and glycerophosphate on Ser[69] (magenta). The structure is displayed with the Pymol software (www.pymol.org). (**F**) Positively charged environment of Ser[93] on the structure of PilE corresponding to the area outlined in (E). A patch of five lysine (K) residues indicated in blue surround Ser[93] in red. (**G**) Predicted structure of the pilin modified with PG on Ser[93].

increased pilin glycerophosphorylation on detachment, we determined the number of bacteria disengaging from microcolonies over time. A laminar flow chamber was used as a tool to progressively collect detaching bacteria (Fig. 4E and fig. S7A). Whereas the number of wild-type bacteria released from the infected monolayer slowly increased with time after 3 hours of infection, detachment of the Δ*pptB* mutant was impaired (1.5×10^6 versus 3.4×10^5 bacteria per ml at 7 hours). About 20 to 30% of bacteria adhering at 6 hours detached in the following hours of infection. The increase in pilin glycerophosphorylation thus favors the release of a proportion of individual bacteria from the microcolonies that has little impact on the number of adhering bacteria.

Bacteria released from microcolonies are more likely to cross the epithelium (*17*), and we tested the ability of the Δ*pptB* mutant to transmigrate across an epithelial cell monolayer (Fig. 4F and fig. S7). After 6 hours, the Δ*pptB* strain had crossed the monolayer 20-fold less efficiently than the wild-type strain, indicating a defect as strong as the nonpiliated *pilE* strain. The strain expressing a point mutation on Ser^{93} of the pilin exhibited a similar defect, showing that the effect of the *pptB* deletion was mediated by the

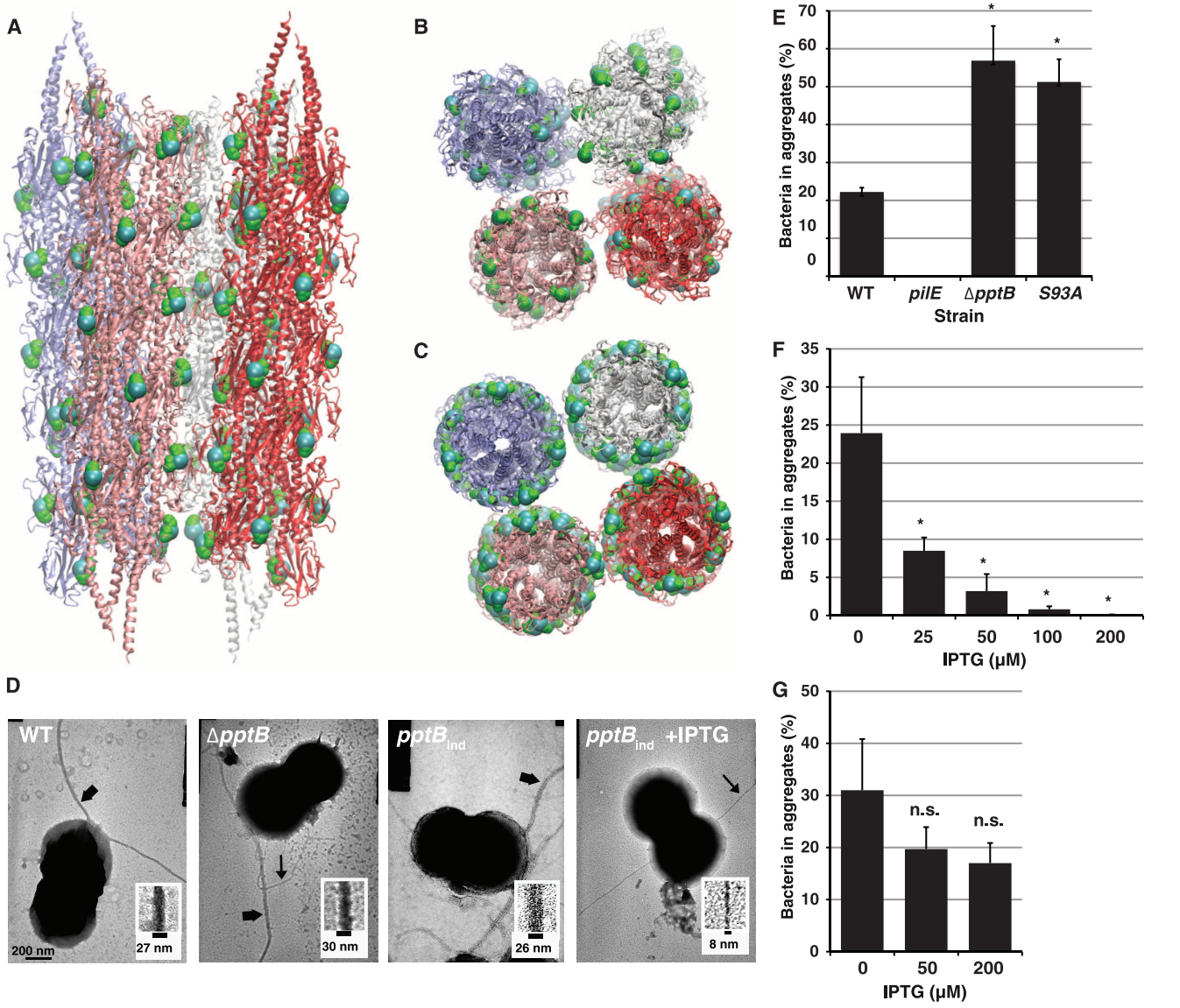

Fig. 3. Effect of pilin glycerophosphorylation on the aggregative functions of type IV pili. (**A** to **C**) Molecular modeling of pili fibers interacting with each other in a bundle. We modeled a regular antiparallel bundle involving four pili fibers by a combination of systematic and random search in the distance between pili, the rotation, and the tilt of the pilus from the overall bundle axis and analyzed them in terms of their interaction energy and the geometry. Each pilus fiber contains 20 monomers of the pilin subunit. (A) Side view of the bundle formed by pilin subunits displaying a PG only on Ser^{69}. The PG modifications are displayed as spheres, phosphate atoms in blue and carbon atoms in green. (B) Top view of the structure shown in (A), showing the close contacts between the fibers. (C) Top view of the unstable bundle that would be formed by the pilin modified with PG on both Ser^{69} and Ser^{93}. (**D**) Effect of increased pilin phosphorylation on the organization of pilus fibers analyzed by transmission electron microscopy for the WT strain, the Δ*pptB* strain, and the $pptB_{ind}$ strain with and without 0.1 mM IPTG. Wide arrows indicate thick bundles of fibers, and narrow arrows indicate thin fibers likely to be individual pili (6 to 8 nm). Insets represent a higher magnification of pili fibers. (**E** to **G**) The ability of bacteria to form aggregates was determined by a technique based on direct observation by fluorescence microscopy. The percentage of bacteria engaged in an aggregate relative to the total amount of bacteria in the same volume is indicated. Four independent experiments each done in triplicate were performed; error bars denote mean ± SEM. Statistical analyses were done with Student's *t* test; n.s., nonsignificant; $*P < 0.05$. (E) Aggregation was compared between the WT strain, the nonpiliated *pilE* strain, the Δ*pptB* strain, and the pilES93A strain. (F) Aggregation was determined in the $pptB_{ind}$ strain in the presence of different amounts of IPTG. (G) Effect on aggregation of increased *pptB* expression in a mutant expressing the PilE protein with an alanine on position 93 ($pptB_{ind}$*PilES93A*).

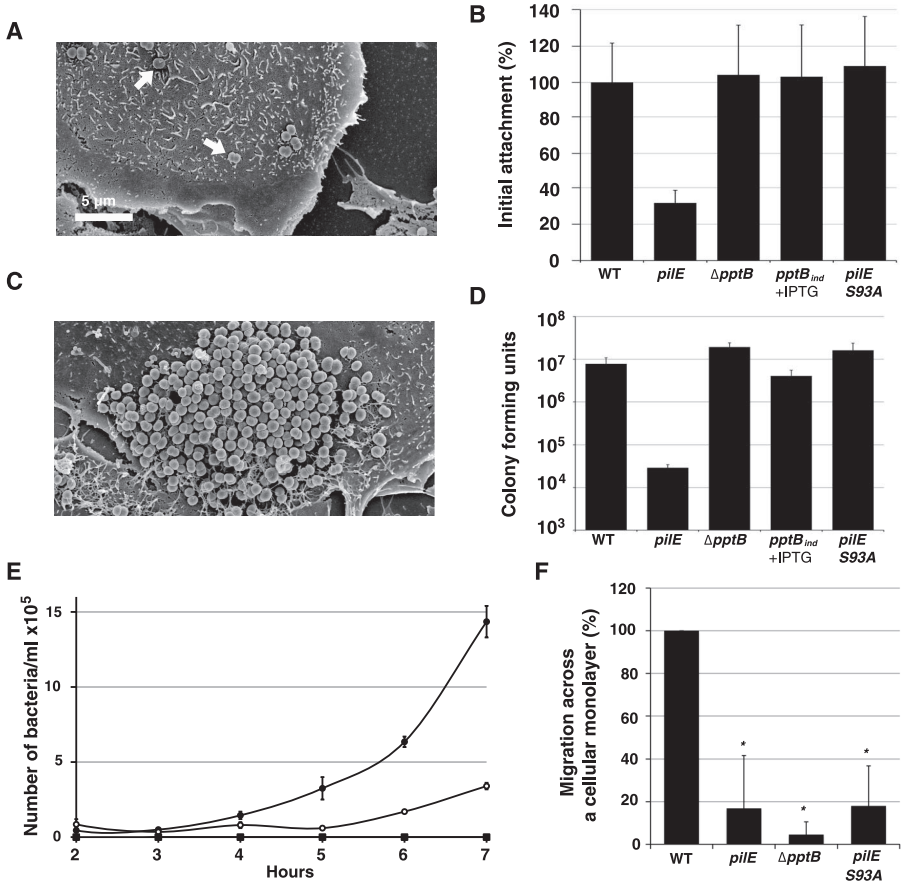

Fig. 4. Effect of pilin glycerophosphorylation on the interaction with host cells. (**A**) Initial adhesion occurs with individual or small groups of bacteria as viewed by scanning electron microscopy (arrows point to a diplococcus). (**B**) Initial binding of individual bacteria to the cellular surface was determined by taking advantage of a flow chamber assay. In the presence of low-intensity flow (0.05 dynes/cm^2), adhering green fluorescent protein–expressing bacteria can be easily distinguished from bacteria in suspension that follow the liquid movement. Results are indicated as the percentage of adhesion relative to the WT strain. (**C**) After initial adhesion, bacteria proliferate and form large bacterial aggregates known as microcolonies. (**D**) Adhesive properties of the different strains to epithelial cells in static conditions were determined by standard dilution plating assays after 6 hours of infection. The transcription of the *pptB* gene was induced in the *pptB$_{ind}$* strain with 0.1 mM IPTG after initial adhesion. (**E**) The number of bacteria detaching from microcolonies adhering to host cells was determined for the wild type and the Δ*pptB* mutant over time by collecting bacteria coming out of a flow chamber submitted to low-intensity flow (0.15 dynes/cm^2). The experiment was performed in parallel for the WT strain (solid circles) and for the Δ*pptB* mutant (open circles). Results for the nonadherent Δ*pilC1* strain are also included (squares). (**F**) The ability of the different strains to transmigrate across an epithelial cell monolayer for a period of 1.5 hours was determined after a 4.5-hour infection period. Results are presented as a percentage relative to wild type. Three independent experiments each done in triplicate were performed; in (B) and (F), error bars denote mean of three experiments ± SEM; in (D) and (E), representative experiments are shown. Statistical analyses were done with Student's *t* test; $*P < 0.05$.

modification of pilin on Ser^{93}. PG modification of Ser^{93} is thus necessary for efficient transmigration across an epithelial barrier.

After several rounds of *N. meningitidis* division on the host cell surface, transcription of the *pptB* gene increases, the major pilin becomes increasingly modified with PG, bacteria lose their aggregative properties, and a small proportion of bacteria are released from the colonies (fig. S8). At the molecular level, pilin glycerophosphorylation on Ser^{93} introduces a steric hindrance and a negative charge in the center of a positively charge patch on pili surface, leading to an inhibitory effect on pili bundling and thus blocking bacterial aggregation. Overall, this process has several potential selective advantages for the bacterium, including transmission to new hosts and colonization of new sites in the same host, thus avoiding nutrient exhaustion and possibly favoring escape from the local immune surveillance. Through a regulated posttranslational modification, *N. meningitidis* adopts a multiply-and-run strategy, presumably selected and fine-tuned through evolution as a propagation mechanism, key for survival of the bacterium in nature. Because selection of this property in the context of the commensal lifestyle of the bacteria also favors transmigration across the epithelium, it is likely to affect human health by favoring invasive infections.

References and Notes

1. M. van Deuren, P. Brandtzaeg, J. W. van der Meer, *Clin. Microbiol. Rev.* **13**, 144 (2000).
2. V. Pelicic, *Mol. Microbiol.* **68**, 827 (2008).
3. G. Mikaty *et al.*, *PLoS Pathog.* **5**, e1000314 (2009).
4. F. T. Hegge *et al.*, *Proc. Natl. Acad. Sci. U.S.A.* **101**, 10798 (2004).
5. E. Stimson *et al.*, *Biochem. J.* **316**, 29 (1996).
6. M. J. Warren, M. P. Jennings, *Infect. Immun.* **71**, 6892 (2003).
7. F. E. Aas *et al.*, *J. Biol. Chem.* **281**, 27712 (2006).
8. J. Chamot-Rooke *et al.*, *Proc. Natl. Acad. Sci. U.S.A.* **104**, 14783 (2007).
9. C. Rusniok *et al.*, *Genome Biol.* **10**, R110 (2009).
10. Materials and methods are available as supporting material on *Science* Online.
11. R. L. Tatusov, E. V. Koonin, D. J. Lipman, *Science* **278**, 631 (1997).
12. S. Morelle, E. Carbonnelle, X. Nassif, *J. Bacteriol.* **185**, 2618 (2003).
13. A. E. Deghmane *et al.*, *EMBO J.* **19**, 1068 (2000).
14. A. Jamet *et al.*, *Microbiology* **155**, 2288 (2009).
15. L. Craig *et al.*, *Mol. Cell* **23**, 651 (2006).
16. M. Marceau, J. L. Beretti, X. Nassif, *Mol. Microbiol.* **17**, 855 (1995).
17. D. Ilver, H. Källström, S. Normark, A. B. Jonsson, *Infect. Immun.* **66**, 469 (1998).

18. Authors thank M.-C. Prévost, S. Guadagnini, D. Lankar, J.-L. Beretti, M. Dupuis, G. Guilbaud for help with experiments and A.-M. Lennon, E. Camerer, S. Silva, and K. Melican for critical reading of the manuscript. This work was supported by Centre National de la Recherche Scientifique, Institut National de la Santé et de la Recherche (including Avenir program), and Agence Nationale de la Recherche grants PCV08_319010 and FRM INE20100118195.

Supporting Online Material

www.sciencemag.org/cgi/content/full/331/6018/778/DC1
Materials and Methods
Figs. S1 to S8
References

22 November 2010; accepted 5 January 2011
10.1126/science.1200729